MIT Open Access Articles

Antibodies specifically targeting a locally misfolded region of tumor associated EGFR

The MIT Faculty has made this article openly available. ***Please share*** how this access benefits you. Your story matters.

Citation	Garrett, Thomas P. J et al. "Antibodies specifically targeting a locally misfolded region of tumor associated EGFR." Proceedings of the National Academy of Sciences 106.13 (2009): 5082-5087. Print.
As Published	http://dx.doi.org/10.1073/pnas.0811559106
Publisher	National Academy of Sciences
Version	Final published version
Citable link	http://hdl.handle.net/1721.1/50256
Terms of Use	Article is made available in accordance with the publisher's policy and may be subject to US copyright law. Please refer to the publisher's site for terms of use.

Massachusetts Institute of Technology

DSpace@MIT

Antibodies specifically targeting a locally misfolded region of tumor associated EGFR

Thomas P. J. Garrett[a,1], Antony W. Burgess[b,1,2], Hui K. Gan[c], Rod B. Luwor[c], Glenn Cartwright[c], Francesca Walker[b], Suzanne G. Orchard[b], Andrew H. A. Clayton[b], Edouard C. Nice[b], Julie Rothacker[b], Bruno Catimel[b], Webster K. Cavenee[d], Lloyd J. Old[e], Elisabeth Stockert[e,3], Gerd Ritter[e], Timothy E. Adams[f], Peter A. Hoyne[f], Dane Wittrup[g], Ginger Chao[g], Jennifer R. Cochran[g], Cindy Luo[a], Mezhen Lou[a], Trevor Huyton[a], Yibin Xu[a], W. Douglas Fairlie[a], Shenggen Yao[a], Andrew M. Scott[c], and Terrance G. Johns[c,4]

[a]Walter and Eliza Hall Institute of Medical Research, Parkville 3050, Australia; [b]Ludwig Institute for Cancer Research, Melbourne Branch, Parkville 3050, Australia; [c]Ludwig Institute for Cancer Research, Melbourne Centre, Heidelberg 3084, Australia; [d]Ludwig Institute for Cancer Research, University of California at San Diego, La Jolla, CA 92093-0660; [e]Ludwig Institute for Cancer Research, New York, NY 10021-6007; [f]Division of Molecular and Health Technologies, Commonwealth Scientific and Industrial Research Organisation, Parkville 3052, Australia; and [g]Department of Chemical Engineering, Massachusetts Institute of Technology, Cambridge, MA 02139

Edited by Jerry M. Adams, The Walter and Eliza Hall Institute of Medical Research, Melbourne, Australia and approved February 17, 2009 (received for review November 19, 2008)

Epidermal Growth Factor Receptor (EGFR) is involved in stimulating the growth of many human tumors, but the success of therapeutic agents has been limited in part by interference from the EGFR on normal tissues. Previously, we reported an antibody (mab806) against a truncated form of EGFR found commonly in gliomas. Remarkably, it also recognizes full-length EGFR on tumor cells but not on normal cells. However, the mechanism for this activity was unclear. Crystallographic structures for Fab:$EGFR_{287–302}$ complexes of mAb806 (and a second, related antibody, mAb175) show that this peptide epitope adopts conformations similar to those found in the wtEGFR. However, in both conformations observed for wtEGFR, tethered and untethered, antibody binding would be prohibited by significant steric clashes with the CR1 domain. Thus, these antibodies must recognize a cryptic epitope in EGFR. Structurally, it appeared that breaking the disulfide bond preceding the epitope might allow the CR1 domain to open up sufficiently for antibody binding. The $EGFR_{C271A/C283A}$ mutant not only binds mAb806, but binds with 1:1 stoichiometry, which is significantly greater than wtEGFR binding. Although mAb806 and mAb175 decrease tumor growth in xenografts displaying mutant, overexpressed, or autocrine stimulated EGFR, neither antibody inhibits the in vitro growth of cells expressing wtEGFR. In contrast, mAb806 completely inhibits the ligand-associated stimulation of cells expressing $EGFR_{C271A/C283A}$. Clearly, the binding of mAb806 and mAb175 to the wtEGFR requires the epitope to be exposed either during receptor activation, mutation, or overexpression. This mechanism suggests the possibility of generating antibodies to target other wild-type receptors on tumor cells.

cancer | cryptic | epitope | therapeutic antibody | structure

Epidermal Growth Factor Receptor (EGFR) activation is a feature of many cancers, but understanding how ligand activates the EGFR has been challenging. However, elegant genetic, biophysical, and crystallographic studies have revealed many of the complex series of conformational changes and aggregation events required to activate the EGFR intracellular tyrosine kinase domain (1, 2). Amidst these complexities, it is apparent that in solution the EGFR extracellular domain adopts at least 2 fundamental conformations: an inactive tethered conformation and an active untethered, or extended, ligand-bound "back-to-back" dimer.

Two major classes of agents have been developed to target the EGFR and prevent receptor activation: tyrosine kinase inhibitors (TKIs) and mAbs (3). TKIs, such as gefitinib and erlotinib, act by competitively binding to the ATP pocket of EGFR (3), whereas mAbs, such as cetuximab (4) and panitumumab (5), inhibit ligand binding. Both classes of agents display significant anti-tumor activity in a range of EGFR-dependent mouse xenograft models, and both have been approved for clinical use in selected cancer patients, including lung, head and neck, and colon cancers, where they display modest activity (3, 6–8). Although these therapeutics show promise, their use is restricted by antibody clearance by wtEGFR in the liver and dose-limiting toxicities, such as skin rash that results from significant uptake of these agents in normal skin where EGFR is expressed (9).

In most gliomas, over-expressed EGFR is associated with the expression of a truncated form of the receptor Δ2–7EGFR (10). The D2–7EGFR contains a unique N-terminal fusion peptide, resulting from the joining of exons 1 and 8. Monoclonal antibodies directed to this junctional peptide have been described (11) and represent potential therapeutics, specific for the tumors that express Δ2–7EGFR. We generated a panel of antibodies against the D2–7EGFR, using NR6 cells over-expressing this truncated EGFR as the immunogen. While binding to the D2–7EGFR, the 2 antibodies described here also bind the over-expressed wtEGFR on cancer cells (12, 13), but notably do not bind to wtEGFR on normal cells. EGFR over-expression and mutation occur in tumor cells but are rare in normal tissues. The results from our completed Phase I clinical trial with a radio-labeled, chimeric version of mAb806 demonstrated that this antibody targets the EGFR on tumors (14). Interestingly, mAb806 also shows synergistic anti-tumor activity in animal models when used in combination with other EGFR therapeutics, including EGFR kinase inhibitors (15) and antibodies to unrelated EGFR epitopes (16). Physiologically and biochemically, this unusual specificity is consistent with the antibodies binding to a cryptic epitope, one not exposed in normal cells but recognizable on cancer cells. Exactly how this specificity is achieved has not been clear.

Epitope mapping studies showed that mAb806 binds a short cysteine loop comprising amino acids 287–302 of the extracellular domain (17). Inspection of crystal structures for this region of

Author contributions: T.P.J.G., A.W.B., L.J.O., T.E.A., and D.W. designed research; T.P.J.G., H.K.G., R.B.L., G. Cartwright, F.W., S.G.O., A.H.A.C., E.C.N., J.R., B.C., W.K.C., E.S., G.R., T.E.A., P.A.H., G. Chao, J.R.C., C.L., M.L., T.H., Y.X., W.D.F., S.Y., and T.G.J. performed research; T.G.J. contributed new reagents/analytic tools; T.P.J.G., A.W.B., F.W., E.C.N., D.W., T.H., S.Y., and A.M.S. analyzed data; and T.P.J.G., A.W.B., and T.G.J. wrote the paper.

The authors declare no conflict of interest.

This article is a PNAS Direct Submission.

Freely available online through the PNAS open access option.

Data deposition: The atomic coordinates and structure factors have been deposited in the Protein Data Bank, www.pdb.org (PDB ID codes 3G5X, 3G5V, and 3G5Y).

[1]T.P.J.G. and A.W.B. contributed equally to this work.

[2]To whom correspondence should be addressed at: Ludwig Institute for Cancer Research, Royal Melbourne Hospital, P.O. Box 2008, Victoria 3050, Australia. E-mail: burgess@ludwig.edu.au.

[3]Deceased September 21, 2002.

[4]Present address: Monash Institute of Medical Research, Clayton 3168, Australia.

This article contains supporting information online at www.pnas.org/cgi/content/full/0811559106/DCSupplemental.

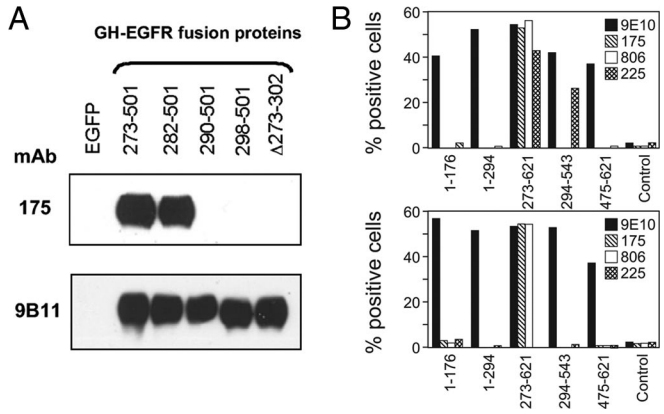

Fig. 1. Localization of the mAb175 epitope in EGFR. (*A*) Lysates from 293T cells transfected with vector control (EGFP) or vectors expressing the EGFR-GH fragment fusion proteins (GH-274–501, GH-282–501, GH-290–501, GH-298–501, and GH-Δ287–302) were resolved by SDS/PAGE, transferred to membrane, and immunoblotted with mAb175 (*Upper*) or the anti-myc antibody 9B11 (*Lower*). (*B*) Fragments of the EGFR were displayed on yeast and their reactivity with mAb175, mAb806, and 2 control antibodies determined by FACS. The epitope recognized by mAb175 is similar to that of mAb806 (*Upper*) and was not sensitive to denaturation by heating yeast pellets to 80 °C for 30 min (*Lower*). The c-myc tag was still recognized by the 9E10 anti-myc antibody in all cases, and the conformation-sensitive EGFR antibody mAb225 was used to confirm denaturation.

wtEGFR suggested that the domain arrangement could prevent access to the epitope in both tethered and untethered forms but access could be possible during ligand activation of the EGFR (17–19). In Δ2–7EGFR, the epitope would be constitutively exposed. In this report, we confirm that mAb175 has the same unusual properties as mAb806. We have also determined the 3D structures for that peptide epitope (EGFR287–302) bound to Fab fragments of 2 antibodies. These studies indicate that the previous molecular interpretation, although plausible, is incorrect. Much of the EGFR surface in contact with the antibodies is buried in the CR1 domain, and EGFR has to locally unfold to bind mAb806 and mAb175. Mutation studies confirm that introducing additional structural instability near the epitope substantially increases epitope access.

Results

Comparison of mAb175 and mAb806 Specificity. Although mAb175 was derived from an independent hybridoma and has a different IgG subtype than mAb806 (IgG2a[a] vs. IgG2b for mAb806), the sequences of the complementarily-determining regions (CDR) were remarkably similar, differing by only one amino acid in each CDR (see supporting information (SI) Fig. S1*A*). Binding analysis for EGFR fragments displayed on yeast established that mAb175 recognized the same fragments as mAb806, thus indicating that part of the epitope resides within amino acids 273–293. Western blots with GH-EGFR fusion fragments refined the epitope within residues 282–293 (Fig. 1 *A* and *B* and Fig. S2). Immunohistochemistry verified that mAb175 detects over-expressed wtEGFR and truncated human EGFR in vivo, but not the wtEGFR when it is expressed at normal levels. mAb175 stained sections of A431 xenografts overexpressing wtEGFR and U87MG cells that express the D2–7EGFR, but not the parental U87MG cells that express only 1×10^5 wtEGFR per cell or sections of normal human liver (Fig. S3). Yeast display of single site mutants within the epitope region showed that residues critical for mAb175 binding were essentially the same for mAb806 (E293, G298, V299, C302 and possibly R300), but that mAb175 appeared moderately more sensitive to mutations at V299 and D297 (Fig. S1*B*).

The affinity of mAb175 for $EGFR_{287–302}$ ranged from 35 nM (Pms-serine coupling) to 154 nM (amine coupling), but, in all cases, the binding affinity of mAb175 for the $EGFR_{287–302}$ peptide was lower than that obtained for mAb806 (Table 1). Conversely, mAb175 bound receptor fragments 1–501 and 1–621 with higher affinity than mAb806 (16 nM vs. 35 nM and 188 nM vs. 389 nM, respectively) (Table 1). For each antibody, the affinity for the full-length extracellular domain, $EGFR_{1–621}$, that can form the tethered conformation was much lower than the untethered form.

Table 1. Antibody affinities for EGFR epitopes

EGFR fragment coupling	K_D for mAb175, nM	K_D for mAb806, nM
287–302 (Pms-Ser)	35 ± 6	16 ± 8
287–302 (Thiol)	143 ± 2	84 ± 3
287–302 (Amine)	154 ± 0.1	85 ± 0.3
1–501* (Amine)	16 ± 0.03	34 ± 0.03
1–621† (Amine)	188 ± 0.01	389 ± 0.01

*Unable to form tether.
†Can form tether.

Efficacy of mAb806 and mAb175 Against Tumor Xenografts Stimulated by Δ2–7EGFR or an EGFR Autocrine Loop. We compared the in vivo anti-tumor activity of mAb806 and mAb175 against U87MG.Δ2–7 glioma xenografts (Fig. 2*A*). Xenografts were allowed to establish for 6 days, and the average tumor volume was 100 mm^3 before antibody therapy commenced. mAb175 treatment inhibited tumor growth more effectively than mAb806 treatment. The average tumor volumes on day 19 were 1530 ± 200 mm^3, 300 ± 30 mm^3, and 100 ± 10 mm^3 for the vehicle, mAb806, and mAb175 treatment groups, respectively ($P < 0.001$ for mAb175 vs. control and $P < 0.002$ for mAb175 vs. mAb806).

Even though U87MG cells express ≈1×10^5 endogenous wtEGFR per cell, mAb806 does not recognize any of the surface EGFR expressed or inhibit the growth of U87MG tumors in vivo

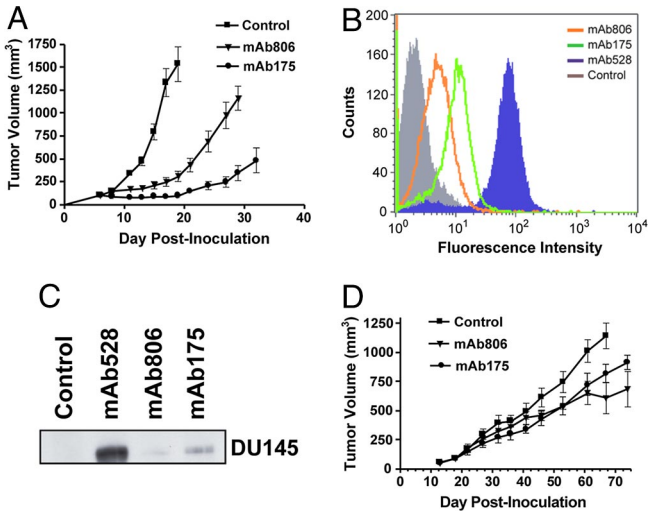

Fig. 2. Effects of mAb175 and mAb806 on glioma and prostate cancer xenografts. (*A*) Mice ($n = 5$) bearing U87MG.Δ2–7 xenografts were injected i.p. with PBS and 1 mg of mAb175 or mAb806 (positive control) on days 6, 8, 10, 13, 15, and 17 when the starting tumor volume was 100 mm^3. Data are expressed as mean tumor volume ± SE. (*B*) DU145 cells were stained with a negative control antibody (gray), mAb528 for total EGFR (blue), mAb806 (orange), and mAb175 (green) and then analyzed by FACS. (*C*) DU145 cells were lysed; subjected to IP with mAb528, mAb806, mAb175, or an independent irrelevant antibody (control); and then immunoblotted for EGFR. (*D*) Mice ($n = 5$) bearing DU145 xenografts were injected i.p. with PBS and 1 mg of mAb175 or mAb806 daily on days 18–22, 25–29, and 39–43 when the starting tumor volume was 90 mm^3. Data are expressed as mean tumor volume ± SE.

BIOCHEMISTRY

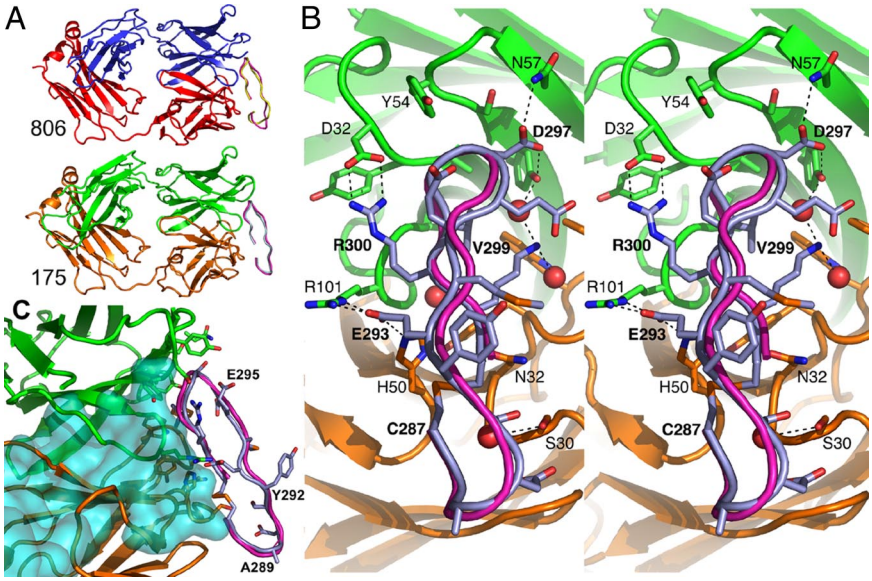

Fig. 3. Crystal structures of EGFR 287–302 bound to the Fab fragments. (*A*) Cartoons of Fab806 (*Upper*), with the light chain (red), heavy chain (blue), bound peptide (yellow), and the superposed $EGFR_{287–302}$ from EGFR (purple) and Fab175 (*Lower*), with the light chain (yellow), heavy chain (green), bound peptide (lilac), and $EGFR_{287–302}$ (purple). (*B*) Detailed stereoview of 175 Fab complex, viewed orthogonal to *A*, looking into the antigen-binding site. Peptide backbones are shown as cartoon and Cα traces and the interacting side chains as sticks (same coloring as in *A*). Atoms are colored as follows: O, red; N, blue; and S, orange; C is as for the main chain and the side chain hydrogen bonds are dashed. Water molecules buried upon complex formation are red spheres. (*C*) Superposition of EGFR (turquoise surface with the 806 epitope displayed as a purple Cα trace) with the Fab175:peptide complex showing spatial overlap (same coloring as in *B*).

(20). U87MG cells do not appear to coexpress any EGFR ligand; however, there is evidence that mAb806 can recognize the EGFR when it is activated by ligand (18). Therefore, we tested whether the wtEGFR could be recognized by mAb806 or mAb175 in cells stimulated by an EGFR autocrine loop (21, 22), such as the prostate cell line DU145. These cells express the wtEGFR at levels similar to that observed in U87MG cells, but contain an amplification of the TGF-α gene (21) and therefore an EGFR/TGF-α autocrine loop. Both mAb175 and mAb806 bind to DU145 cells as determined by FACS analysis (Fig. 2*B*), and both antibodies are able to immunoprecipitate a small proportion of the EGFR extracted from these cells (Fig. 2*C*). In each case, mAb175 binds more effectively than mAb806.

Because mAb175 and mAb806 bind more effectively to the EGFR expressed in DU145 cells than U87MG cells, we analyzed the anti-tumor activity of these antibodies in DU145 xenografts grown in nude mice (Fig. 2*D*). Xenografts were allowed to establish for 18 days to an average tumor volume of 90 mm^3. Therapy consisted of three 1-mg injections per week for 3 weeks on days indicated (Fig. 2*D*). Both mAb175 and mAb806 inhibited the growth of DU145 xenografts. The control group was killed on day 67 and had a mean tumor volume of 1145 ± 100 mm^3 compared with 605 ± 150 mm^3 ($P < 0.007$) and 815 ± 50 mm^3 ($P < 0.02$) for the mAb806 and mAb175 groups, respectively. Surprisingly, both mAb175 and mAb806 inhibited the growth of these xenografts containing low levels of wtEGFR when they were activated by autocrine secretion of ligand.

3D Structure of $EGFR_{287–302}$ with the Fab Fragments of mAb806 and mAb175. To understand the molecular details of how mAb175 and mAb806 recognize a subset of the wtEGFR molecules, crystal structures of Fab fragments for both antibodies were determined alone and in complex with the oxidized epitope, $EGFR_{287–302}$ (at 2.8 Å and 1.59 Å resolution, respectively, for mAb175; and 2.2 Å and 2.0 Å resolution, respectively, for mAb806) (Fig. 3*A* and Table S1). In each case, the structures of each free and complexed Fab were essentially the same and the conformations of $EGFR_{287–302}$ and the CDR loops of the antibodies were well defined. The epitope adopts a β-ribbon structure, with one edge of the ribbon pointing toward the Fab and with V299 buried at the center of the binding site (Fig. 3 *B* and *C*). Both ends of the epitope were exposed to solvent, consistent with the ability of these antibodies to bind to longer EGFR peptides that include $EGFR_{287–302}$.

Of the 20 antibody residues in contact with the epitope, there are only 2 substitutions between mAb806 and mAb175 (Fig. 3 *B* and *C* and Fig. S1*A*). mAb175 contact residues are: light-chain S30, S31, N32, Y49, H50, Y91, F94, and W96 and heavy-chain D32, Y33, A34, Y51, S53, Y54, S55, N57, R59, A99, G100, and R101; the mAb806 contact residues are the same, with sequence differences for the light-chain, N30, and heavy-chain, F33. $EGFR_{287–302}$ binds to the Fab through close contacts between peptide residues 293–302, with most of the contacts being between residues 297 and 302. Main chain atoms of residues 300 and 302 hydrogen bond to the Fab (Fig. 3*C*). Recognition of the epitope sequence occurs through side-chain hydrogen bonds to residues E293 (to H50 and R101 of the Fab), D297 (to Y51 and N57), R300 (to D32), and K301 (via water molecules to Y51 and W96). Hydrophobic contacts are made at G298, V299, and C302. These contacts are consistent with the fine epitope mapping study for mAb806/EGFR that showed that E293, G298, V299, and C302 are important for antibody binding (23).

The conformation of the epitope backbone between amino acids 293 and 302 was essentially identical in the Fab806 and Fab175 crystals (rmsd = 0.4 Å for Cα atoms in these residues). Although it is constrained by the disulfide bond, the N terminus of the peptide (287–292) does not make significant contact in either antibody structure and the conformations of the peptide in this region differ significantly. In the Fab806 complex, this peptide segment appears rather disordered (Fig. 3*A*). More interestingly, the conformation of the $EGFR_{287–302}$ peptide in contact with the antibodies is closely related to the $EGFR_{287–302}$ conformation observed in the backbone of the EGFR structures (24, 25). In the Fab175:$EGFR_{287–302}$ complex, the rmsd in Cα positions to tethered EGFR (25) is 0.66 Å and to untethered EGFR (chain B) (24) is 0.75 Å (Fig. 3 *B* and *C*). We also studied the solution conformation of ^{15}N-labeled oxidized $EGFR_{287–302}$ by NMR spectroscopy. Comparing assigned resonances with those for random coil (Fig. S4), the free peptide adopted essentially a random coil structure, not the β-ribbon as seen in wtEGFR (24), implying that the antibodies induce the wild-type conformation in the peptide epitope.

Why do mAb806 and mAb175 recognize a subset of EGFR conformations? We manually docked the Fab structure of mAb175 onto an extracellular domain of wtEGFR (tethered and untethered monomers) and D2–7EGFR models by superimposing $EGFR_{287–302}$ from the mAb complex on that in the EGFR structures. D2–7EGFR models were made by truncation of the corresponding ectodomain conformer. For the D2–7EGFR, there were no significant steric clashes with the receptor. In the

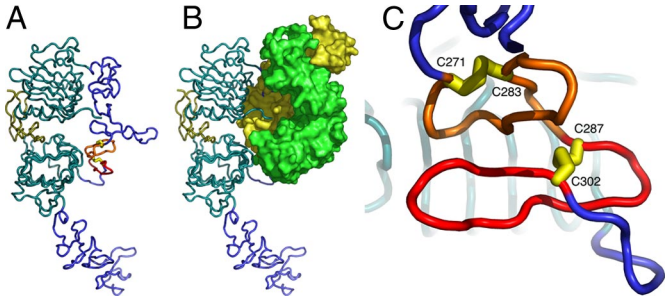

Fig. 4. Location of the mAb806/175 epitope in EGFR. (*A*) Cα trace of the ectodomain for untethered EGFR1–621. L1 is at the top with L1 and L2 in teal, CR1 and CR2 in blue, and TGF-α in olive. The mAb806/175 epitope is drawn in red, with the preceding loop (residues 271–286) in orange and the disulfide bonds in yellow. The model was constructed by docking the EGFR-ECD CR2 domain from the tethered conformation (36) onto the structure of an untethered EGFR monomer in the presence of its ligand (24). (*B*) Untethered EGFR ectodomain (as in *A*) showing the spacial overlap with the mAb175 Fab (solvent contact surface with the light chain in yellow and the heavy chain in green). The Fab was positioned by superimposing the $EGFR_{287–302}$ peptide on the corresponding region of EGFR. The CR1 domain is almost completely buried within the Fab. (*C*) Detail of *A*, viewed from the right, showing how the preceding disulfide-bonded loop blocks access to the epitope.

untethered model of Δ2–7EGFR, there is substantially more accessible surface area of the Fab buried (920 $Å^2$ compared with 550 $Å^2$ in the tethered model), and this conformer appears to make additional contacts with non-CDR regions of the antibody, particularly the L2 domain. In contrast, attempts to dock the whole EGFR ectodomain onto the Fab revealed a substantial spatial overlap of the Fab with the part of the CR1 domain preceding the epitope (Figs. 3*C* and 4 *A* and *B*). Upon superposing $EGFR_{287–302}$ from the untethered form of wtEGFR on the corresponding region Fab complex, almost the entire CR1 domain lies buried within the body of the Fab (Fig. 4 *A* and *B*). Furthermore, because the CR1 domain has essentially the same structure in tethered or untethered conformations, mAb806 or mAb175 would overlap with and not be able to bind to either form of wtEGFR. Therefore, any orientation that permits mAb806 or mAb175 binding must have a different conformation, which reorients the epitope with respect to the CR1 domain. Inspection of the CR1 domain indicated that the disulfide bond (271–283) preceding $EGFR_{287–302}$ constrains the orientation of the polypeptide chain in the region of the epitope in a manner that prevents binding of these antibodies. Disruption of disulfide bond 271–283, even though it is not directly involved in binding to mAb806 and mAb175, would be expected to allow partial unfolding of the CR1 domain and consequently allow access of these antibodies to the 287–302 epitope.

Removing the EGFR 271–283 Disulfide Bond Increases mAb806 Binding. Protein–disulfide bonds usually provide increased structural rigidity, but in some cell surface receptors, particularly those for cytokines and growth factors, transient breaking of disulfide bonds and disulfide exchange can control the receptor's function (26). We mutated either or both of the EGFR cysteine residues at positions 271 and 283 to alanine residues (C271A/C283A). The vectors capable of expressing full-length $EGFR_{C271A}$, $EGFR_{C283A}$, or $EGFR_{C271A/C283A}$ were transfected into the IL-3-dependent BaF/3 cell line. Stable BaF/3 clones that expressed the mutants at normal levels, i.e., $<10^5$ per cell, were selected. The wtEGFR reacts poorly with mAb806; however, all of the cysteine mutants bound mAb806 strongly (Fig. 5*A* and Fig. S5). Because these cysteine mutants also bound mAb528, they must be displayed on the cell surface with at least their L2 domain folded correctly. Quantitatively, mAb806 only recognized a small proportion of the total wtEGFR expressed on the surface of BaF/3 cells (the mAb806/528 binding ratio is 0.07). In contrast, mAb806 recognizes all of the $EGFR_{C271A/C283A}$ displayed on the cell surface (the mAb806/528 binding ratio is 1.01 ± 0.13).

Western blotting analysis confirmed that the $EGFR_{C271A/C283A}$ mutant is expressed at similar levels to the wtEGFR and is tyrosine phosphorylated in response to EGF stimulation (Fig. 5*B*). Further-

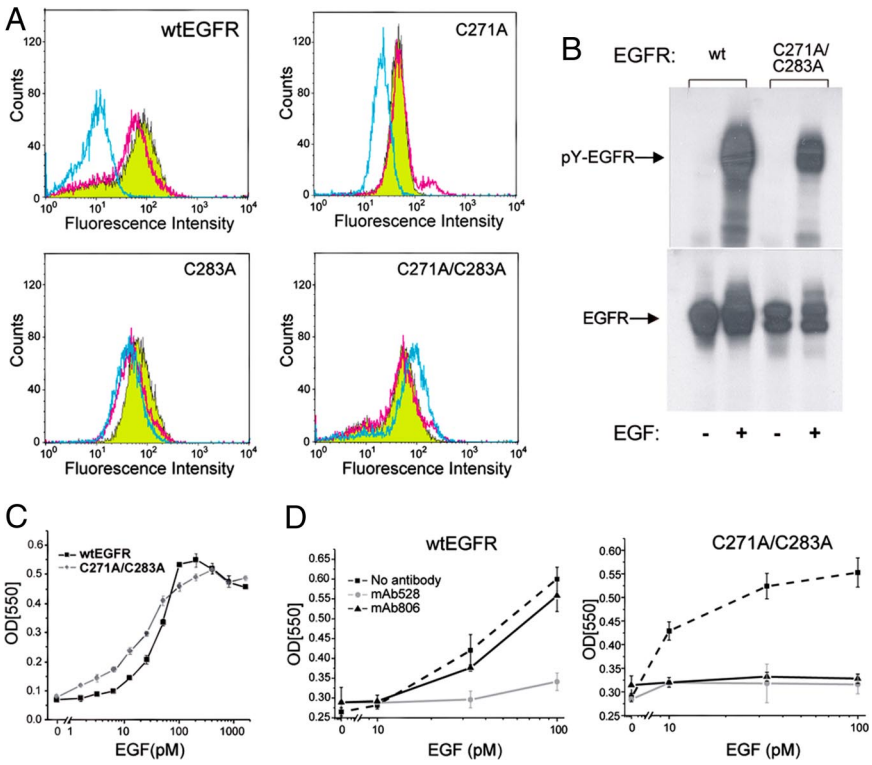

Fig. 5. Influence of the 271–283 cysteine bond on mAb806 binding to the EGFR. (*A*) Cells transfected with wtEGFR or EGFR C271A/C283A were stained with mAb528 (green), mAb806 (cyan), or the anti-FLAG antibody M2 (pink), and then analyzed by FACS. The gain was set using a class-matched irrelevant antibody. (*B*) BaF/3 cells expressing the wtEGFR or the C271A/C283A mutant were IL-3 and serum starved, then exposed to EGF. Whole cell lysates were separated by SDS/PAGE and immunoblotted with anti-phosphotyrosine antibody (*Upper*) or anti-EGFR antibody (*Lower*). (*C*) BaF/3 cells expressing wtEGFR or the C271A/C283A mutant were examined for their response to EGF in an MTT assay. EC_{50} = 51 and 20 pM for wtEGFR and C271A/C283A mutant, respectively, with values derived using a Boltzman fit of the data points. Data represent mean ± SD of triplicate measurements. (*D*) BaF/3 cells expressing wtEGFR or EGFR-C271A/C283A were stimulated with increasing concentrations of EGF either in the absence of antibody or presence of mAb528 or mAb806, both at 10 μg/mL. Data are expressed as mean ± SD of triplicate measurements.

BIOCHEMISTRY

more, mutation of the 2 cysteines did not compromise EGF binding or receptor function: BaF/3 cells expressing the $EGFR_{C271A/C283A}$ mutant proliferate in the presence of EGF (Fig. 5*C*). We have reproducibly observed that the BaF/3 cells expressing the $EGFR_{C271A/C283A}$ mutation respond to lower concentrations of EGFR, suggesting either higher affinity for the ligand or enhanced signaling potential for the mutant receptor. mAb806 has no effect on the in vitro EGF-induced proliferation of Ba/F3 wtEGFR cells, whereas mAb528 strongly inhibited the EGF-induced proliferation of these cells (Fig. 5*D Left*). In contrast, mAb806 totally ablated the EGF-induced proliferation in BaF3 $EGFR_{C271/283A}$ cells (Fig. 5*D Right*).

Discussion

When the EGFR or erbB2 are over-expressed or mutated in tumors, antibodies such as cetuximab, panitumumab, and herceptin that target EGFR family members are important options for treatment (3). The 3D structures of both the target receptor (1) and the antibody:receptor complexes (25, 27, 28) have improved our understanding of how these antibodies interfere with receptor activation. Studies such as these have also suggested that targeting other epitopes on this receptor family may produce new opportunities for using combinations of antibodies to improve cancer treatment. A drawback, however, with all currently approved therapeutic anti-EGFR antibodies is that they recognize the wtEGFR that is expressed in normal tissues including skin, liver, and gut. Not only does this pool of EGFR in normal tissue represent a large sink for the antibodies, it makes the use of antibody/cytotoxic conjugates impractical. Despite these limitations, it should be noted that the EGFR in many normal tissues (e.g., liver) appears not to be activated, so neutralizing anti-EGFR antibodies do not have a profound effect on vital homeostatic signaling (29). Many tumors contain over-expressed, mutated, or activated EGFR. Importantly, activated EGFR is functionally involved in the maintenance of the tumorgenicity state by enhancing cell movement, proliferation, invasion, angiogenesis, and survival of tumor cells. Consequently, the administration of anti-EGFR antibodies or EGFR kinase inhibitors can decrease the growth and survival of the tumor cells.

Antibodies directed to the unique junctional peptide in the D2–7EGFR have the potential to target several tumor types, including glioma (29), without the difficulties associated with normal tissue uptake. However, the expression of the D2–7EGFR is infrequent, compared with over-expression of the wtEGFR, and antibodies targeting just Δ2–7EGFR will not necessarily inhibit over-expressed wtEGFR (30). mAb806 and mAb175 not only bind this truncated receptor, but also bind to over-expressed wtEGFR. These antibodies recognize an epitope contained within a cysteine loop (amino acids 287–302) that is accessible in the D2–7EGFR, but not in the wtEGFR, when expressed at low to moderate levels on cells in the absence of ligands (13). A previous attempt to predict how mAb806 bound its epitope in the context of the EGFR was not successful (19). Despite the generation of 3 models, the unusual change in accessibility of the epitope confounded the prediction algorithms, so it was not possible to use the predicted structures to improve our understanding of mAb806 binding to the wtEGFR.

Our structural studies with the $EGFR_{287–302}$ epitope show that both mAb806 and mAb175 recognized the same 3D structural motif in the wtEGFR structures (24, 25), suggesting that this backbone conformation also occurs in and is exposed in the D2–7EGFR. Critically, however, the orientation of the epitope in these structures would prevent antibody access to the relevant amino acids. This orientation is consistent with the experimental observation that mAb806 does not bind wtEGFR expressed on the cell surface at physiological levels. Detailed inspection of the EGFR structure raised another intriguing possibility. The $EGFR_{287–302}$ epitope lies against a second disulfide-bonded loop (amino acids 271–283), and we predicted that the disruption of this disulfide bond would allow access to the $EGFR_{287–302}$ loop without changing its backbone conformation (Fig. 4). Our results with the $EGFR_{C271A/C283A}$ mutant indicate that the CR1 domain can open up to allow mAb806 and mAb175 to bind stoichiometrically to this mutant receptor. This mutant receptor can still adopt a native conformation because it is fully responsive to EGF stimulation but, unlike the wtEGFR, is fully inhibited by mAb806. If a misfolded form of the EGFR with this disulfide bond broken were to exist on the surface of cancer cells, our data clearly shows it would be capable of initiating cell signaling and should be inhibited by either mAb806 or mAb175.

There is a second potentially more likely possibility to explain the binding of these antibodies. During ligand activation, the structural rearrangement of the receptor could induce local unfolding in the vicinity of the epitope, allowing the receptor to adopt a conformation that permits binding. In crystal structures, the epitope lies near the physical center of the EGFR ectodomain and access to the epitope is blocked by both the folded CR1 domain and the quaternary structure of the EGFR ectodomain. In the tethered and the untethered conformations, the integrity of the CR1 domain is stabilized by additional interactions with either the L1:ligand:L2 domains (untethered) or the L2:CR2 domains (tethered). However, the epitope region has some of the highest thermal parameters found in the ectodomain; the mAb806/175 epitope is structurally labile. During receptor activation, when the receptor undergoes a transition between the tethered and untethered conformations, it appears that mAb806 and mAb175 can access the epitope. Thus, at the molecular level, these mechanisms could contribute to the negligible binding of mAb806 and mAb175 to normal cells and the substantially higher levels of binding to tumor cells that have overexpressed and/or activated EGFR.

The mAb806 and mAb175 reactivity to a locally misfolded region of its target protein suggests the possibility of generating antibodies to other overexpressed/misfolded receptors for cancer therapeutics. For other members of the EGFR family, one approach would be to use the disulfide mutants equivalent to $EGFR_{C227A/C283A}$ as immunogens because this would increase exposure of the equivalent epitope in an appropriately folded form. Under glycosylation or kinase, mutations of EGFR also increase mAb806 epitope accessibility and would provide alternate immunization strategies. More generally, in tumor cells that overexpress other growth factor receptors, in particular receptors with disulfide-rich domains (e.g., the insulin-like growth factor receptors (IGFRs), we predict that a proportion of these receptors will be partially misfolded because of factors such as under glycosylation or transiently mismatched or unformed disulfide bonds. Thus, it is conceivable that other disulfide mutant or truncated receptors could be used as immunogens to generate tumor-specific anti-receptor antibodies for use in cancer treatment.

Materials and Methods

Cell Lines. The Δ2–7EGFR transfected U87MG.Δ2–7 (10), the A431 (31), and the hormone-independent prostate DU145 (21) cell lines were grown as previously described (16). For site-directed mutants, BaF/3 cell lines expressing different EGF receptors were maintained as reported earlier (32).

Antibodies, Fabs, and Peptides. Sequences of the mAb variable domains were determined from cDNAs, with corrections from the crystal structures. mAb806 and mAb175 were produced in the Ludwig Institute for Cancer Research Biological Production Facility, Melbourne. Intact mAbs were digested with activated papain at 37 °C at a ratio of 1:20 and the papain inactivated with iodoacetamide. The digestion was passed over Protein-A Sepharose (Amersham) with the flow-through further purified by cation exchange using a Mono-S column (Amersham) and concentrated using a 10,000 molecular weight cutoff (MWCO) centrifugal concentrator (Millipore). For Fab–peptide complexes, a molar excess of lyophilized peptide was added directly to the Fab and incubated for 2 h at 4 °C before setting up crystallization trials. The $EGFR_{287–302}$ was synthesized using Fmoc chemistry, purified by RP-HPLC, and characterized by MS analysis.

Immunoprecipitation and Western Blotting. Cells were lysed using 1% Triton X-100, 30 mM Hepes, 150 mM NaCl, 500 mM 4-(2-aminoethyl) benzenesulfonylfluoride, 150 nM aprotinin, 1 mM E-64 protease inhibitor, 0.5 mM EDTA, and 1 mM leupeptin (pH 7.4) for 20 min, clarified by centrifugation at 14,000 $\times$ *g* for 30 min, immunoprecipitated with the relevant antibodies at a final concentration of 5 μg/mL for 60 min, and captured by Sepharose-A beads overnight. Samples were then eluted with 2X NuPAGE SDS Sample Buffer (Invitrogen), resolved on NuPAGE gels, electro-transferred onto Immobilon-P transfer membrane (Millipore), and then probed with the relevant antibodies before detection by chemoluminescence radiography.

Surface Plasmon Resonance. Using BIAcore 3000, EGFR fragments were immobilized on a CM5 sensor chip using amine, thiol, or Pms coupling at a flow rate of 5 μL/min (33). The mAb806 and mAb175 were passed over the sensor surface at a flow rate of 5 μL/min at 25 °C. K_D values were calculated from equilibrium binding data obtained by passing different concentrations of antibody over the sensor surfaces. Equilibrium binding data were analyzed in Scatchard format [Req/C vs. Req, where Req is the sensorgram signal at equilibrium and C is the concentration (nM)]. The data were fitted using linear regression.

Xenograft Models. U87MG.Δ2–7 or DU145 cells (3×10^6) in 100 μL of PBS were inoculated s.c. into both flanks of 4- to 6-week-old female BALB/c nude mice (Animal Research Centre). All studies were conducted using established tumor models as reported previously (16). Data are expressed as mean tumor volume $\pm$ SE for each treatment group. Data were analyzed for significance by one-sided Student's *t* test where $P < 0.05$ was considered statistically significant. This research project was approved by the Animal Ethics Committee of the Austin Health, Heldelberg, Australia.

Generation and Characterization of Stable Cell Lines Expressing EGFR Mutant Constructs. The template for each mutagenesis was the human wtEGFR cDNA (GenBank accession number x00588) (31). Mutations were generated using a site-directed mutagenesis kit (Stratagene) and verified by automated nucleotide sequencing of each construct. Wild-type and mutant (C173, C281, and C173A/C281A) EGFR were transfected into BaF/3 cells by electroporation, and stable cell lines were obtained as described previously (18). Methods for FACS analysis, EGF induced proliferation assays, and analysis of EGFR activation by immunoblotting of Ba/F3 cells expressing variants of the EGFR have been extensively described in earlier manuscripts (18, 24).

Crystal Structure Determinations. Crystals were grown using a Topaz crystallization system (Fluidigm) and by hanging drop vapor diffusion from a 1:1 mixture of protein (7–10 mg/mL) and precipitant solutions, comprising: 0.15 M sodium formate and 15% PEG1500 for Fab175:peptide; 0.2 M ammonium acetate 16–18% PEG5000 monomethylether for the Fab806:peptide; 0.4 M NaI, 16% PEG6000, 0.1 M Mes at pH 6.0 for Fab175 alone; 0.1 M sodium acetate at pH 4.6, 6–8% PEG6000, and 15–20% isopropanol for Fab806. Further details are in SI. Just before data collection, crystals were transferred to a cryoprotectant solution, consisting of reservoir supplemented with 25% glycerol (10% for Fab806 and 3% additional PEG6000), then mounted in a nylon loop and flash frozen directly into liquid nitrogen.

Diffraction data were collected using a Rigaku R-AXIS IV detector on a Micromax-007 generator fitted with AXCO optics or at beamline X29, NSLS synchrotron, and processed with CrystalClear or HKL2000, respectively. Structures were solved by molecular replacement with MOLREP (34), using pairs of V or C domains from PDB:12E8 for Fab806 alone, then Fab806 for the other structures. Refinement with REFMAC5 (35) converged with R = 0.216 and R_{free} = 0.281 for Fab806, R = 0.211 and R_{free} = 0.273 for Fab806:peptide, R = 0.210 and R_{free} = 0.305 for Fab175, and R = 0.199 and R_{free} = 0.250 for Fab175:peptide. Data statistics are shown in Table S1.

ACKNOWLEDGMENTS. We thank Colin Ward for valuable advice; Peter Czabotar, Marc Kvansakul, and Peter Colman for collecting some data at the National Synchrotron Light Source (NSLS), Upton, NY; the staff at beamline X29 for their assistance; and the Australian Synchrotron Research Program and the U.S. Department of Energy for providing access. This work was supported in part by National Health and Medical Research Council Program Grant 280912 and Project Grant 433615 and National Institutes of Health Grant CA96504. W.D.F. and T.P.J.G. are supported by National Health and Medical Research Council Fellowships. W.K.C. is supported in part by National Cancer Institute-National Institutes of Health Grant CA95616 and is a fellow of the National Foundation for Cancer Research.

1. Burgess AW, et al. (2003) An open-and-shut case? Recent insights into the activation of EGF/ErbB receptors. *Mol Cell* 12:541–552.
2. Ferguson KM (2008) Structure-based view of epidermal growth factor receptor regulation. *Annu Rev Biophys* 37:353–373.
3. Mendelsohn J, Baselga J (2006) Epidermal growth factor receptor targeting in cancer. *Semin Oncol* 33:369–385.
4. Herbst RS, Kim ES, Harari PM (2001) IMC-C225, an anti-epidermal growth factor receptor monoclonal antibody, for treatment of head and neck cancer. *Expert Opin Biol Ther* 1:719–732.
5. Lynch DH, Yang XD (2002) Therapeutic potential of ABX-EGF: A fully human anti-epidermal growth factor receptor monoclonal antibody for cancer treatment. *Semin Oncol* 29:47–50.
6. Baselga J, Arteaga CL (2005) Critical update and emerging trends in epidermal growth factor receptor targeting in cancer. *J Clin Oncol* 23:2445–2459.
7. Burgess AW (2008) EGFR family: Structure physiology signalling and therapeutic targets. *Growth Factors* 26:263–274.
8. Milano G, Spano JP, Leyland-Jones B (2008) EGFR-targeting drugs in combination with cytotoxic agents: from bench to bedside, a contrasted reality. *Br J Cancer* 99:1–5.
9. Solomon BM, Jatoi A (2008) Rash from EGFR inhibitors: Opportunities and challenges for palliation. *Curr Oncol Rep* 10:304–308.
10. Nishikawa R, et al. (1994) A mutant epidermal growth factor receptor common in human glioma confers enhanced tumorigenicity. *Proc Natl Acad Sci USA* 91:7727–7731.
11. Humphrey PA, et al. (1990) Anti-synthetic peptide antibody reacting at the fusion junction of deletion-mutant epidermal growth factor receptors in human glioblastoma. *Proc Natl Acad Sci USA* 87:4207–4211.
12. Johns TG, et al. (2002) Novel monoclonal antibody specific for the de2–7 epidermal growth factor receptor (EGFR) that also recognizes the EGFR expressed in cells containing amplification of the EGFR gene. *Int J Cancer* 98:398–408.
13. Jungbluth AA, et al. (2003) A monoclonal antibody recognizing human cancers with amplification/overexpression of the human epidermal growth factor receptor. *Proc Natl Acad Sci USA* 100:639–644.
14. Scott AM, et al. (2007) A phase I clinical trial with monoclonal antibody ch806 targeting transitional state and mutant epidermal growth factor receptors. *Proc Natl Acad Sci USA* 104:4071–4076.
15. Johns TG, et al. (2003) Antitumor efficacy of cytotoxic drugs and the monoclonal antibody 806 is enhanced by the EGF receptor inhibitor AG1478. *Proc Natl Acad Sci USA* 100:15871–15876.
16. Perera RM, et al. (2005) Treatment of human tumor xenografts with monoclonal antibody 806 in combination with a prototypical epidermal growth factor receptor-specific antibody generates enhanced antitumor activity. *Clin Cancer Res* 11:6390–6399.
17. Johns TG, et al. (2004) Identification of the epitope for the epidermal growth factor receptor-specific monoclonal antibody 806 reveals that it preferentially recognizes an untethered form of the receptor. *J BiolChem* 279:30375–30384.
18. Walker F, et al. (2004) CR1/CR2 interactions modulate the functions of the cell surface epidermal growth factor receptor. *J BiolChem* 279:22387–22398.
19. Sivasubramanian A, et al. (2006) Structural model of the mAb 806-EGFR complex using computational docking followed by computational and experimental mutagenesis. *Structure* 14:401–414.
20. Luwor RB, et al. (2001) Monoclonal antibody 806 inhibits the growth of tumor xenografts expressing either the de2–7 or amplified epidermal growth factor receptor (EGFR) but not wild-type EGFR. *Cancer Res* 61:5355–5361.
21. Ching KZ, et al. (1993) Expression of mRNA for epidermal growth factor, transforming growth factor-alpha and their receptor in human prostate tissue and cell lines. *Mol Cell Biochem* 126:151–158.
22. Sizeland AM, Burgess AW (1991) The proliferative and morphologic responses of a colon carcinoma cell line (LIM 1215) require the production of two autocrine factors. *Mol Cell Biol* 11:4005–4014.
23. Chao G, Cochran JR, Wittrup KD (2004) Fine epitope mapping of anti-epidermal growth factor receptor antibodies through random mutagenesis and yeast surface display. *J Mol Biol* 342:539–550.
24. Garrett TP, et al. (2002) Crystal structure of a truncated epidermal growth factor receptor extracellular domain bound to transforming growth factor alpha. *Cell* 110:763–773.
25. Li S, et al. (2005) Structural basis for inhibition of the epidermal growth factor receptor by cetuximab. *Cancer Cell* 7:301–311.
26. Hogg PJ (2003) Disulfide bonds as switches for protein function. *Trends Biochem Sci* 28:210–214.
27. Li S, Kussie P, Ferguson KM (2008) Structural basis for EGF receptor inhibition by the therapeutic antibody IMC-11F8. *Structure* 16:216–227.
28. Schmiedel J, et al. (2008) Matuzumab binding to EGFR prevents the conformational rearrangement required for dimerization. *Cancer Cell* 13:365–373.
29. Sandler AB (2006) Nondermatologic adverse events associated with anti-EGFR therapy. *Oncology (Williston Park)* 20:35–40.
30. Sampson JH, et al. (2000) Unarmed, tumor-specific monoclonal antibody effectively treats brain tumors. *Proc Natl Acad Sci USA* 97:7503–7508.
31. Ullrich A, et al. (1984) Human epidermal growth factor receptor cDNA sequence and aberrant expression of the amplified gene in A431 epidermoid carcinoma cells. *Nature* 309:418–425.
32. Walker F, et al. (1998) Biochemical characterization of mutant EGF receptors expressed in the hemopoietic cell line BaF/3. *Growth Factors* 16:53–67.
33. Wade JD, et al. (2006) An automated peptide and protein thiazolidine coupling chemistry for biosensor immobilization giving a unique N-terminal orientation. *Anal Biochem* 348:315–317.
34. Vagin AA, Isupov MN (2001) Spherically averaged phased translation function and its application to the search for molecules and fragments in electron-density maps. *Acta Crystallogr D Biol Crystallogr* 57:1451–1456.
35. Murshudov GN, Vagin AA, Dodson EJ (1997) Refinement of macromolecular structures by the maximum-likelihood method. *Acta Crystallogr D Biol Crystallogr* 53:240–255.
36. Ferguson KM, et al. (2003) EGF activates its receptor by removing interactions that autoinhibit ectodomain dimerization. *Mol Cell* 11:507–517.